East European Journal of Physics. 3. 643-653 (2026)
DOI: 10.26565/2312-4334-2026-3-60 ISSN 2312-4334

ELECTRONIC STRUCTURE AND INTERMOLECULAR INTERACTIONS OF THE BENZOIC ACID–ETHANOL COMPLEX: RAMAN SPECTROSCOPY, DFT, AND MOLECULAR DOCKING ANALYSIS

Abduvakhid Jumabaev[1], Hakim Hushvaktov[1], Ahmad Absanov[1], Asliddin Norkulov[1], Zokhid Ernazarov[1], Leonid Bulavin[2]
[1]Samarkand State University named after Sharof Rashidov, 15 University Blvd, 140104, Samarkand, Uzbekistan
[2]Taras Shevchenko National University of Kyiv (64/13, Volodymyrska Str., Kyiv 01601, Ukraine
Corresponding Author e-mail: erudni67@gmail.com
Received June 1, 2026; revised August 13, 2026; accepted August 27, 2026

In this work, we investigated intermolecular interactions in benzoic acid and its ethanol solutions using Raman spectroscopy and quantum-chemical approaches. Analysis of the Raman spectra revealed that adding ethanol induces significant changes in benzoic acid's vibrational spectrum. These changes are primarily due to solvent effects and hydrogen-bond formation and are most pronounced in the vibrational modes corresponding to the carboxyl group. The near-invariance of the aromatic ring confirms the preservation of the structural integrity of the molecule. Theoretical calculations were performed at the DFT level, providing a thorough analysis of the system's electronic structure and energetic characteristics. The molecular electrostatic potential (MEP) surface was used to identify reactive sites within the molecule; the oxygen atoms of the carboxyl group emerged as the principal electron-rich nucleophilic centers, while the –OH group of ethanol played a significant role in hydrogen bond formation. HOMO–LUMO orbital analysis demonstrated a redistribution of electron density during complex formation and an increase in the reactivity of the system. Molecular docking results also confirmed benzoic acid's ability to interact with a biologically active binding site. During the calculations, the molecule adopted a stable conformation within the protein's active site, forming a complex through hydrogen bonds and other weak intermolecular interactions. These findings align with the MEP and electronic structure analyses, showing a close link between the molecule's quantum-chemical properties and its potential biological activity. The investigations reveal the mechanism of intermolecular interactions in the benzoic acid–ethanol system and provide a comprehensive explanation of how these interactions influence the molecule's vibrational properties, electronic structure, and behavior in a biological environment.
Key words: *Raman spectroscopy; Ab initio calculations; Hydrogen bonding; Benzoic acid; Ethanol; Molecular electrostatic potential (MEP) surface; AIM; FMO; Molecular docking*

1. INTRODUCTION

One of the main directions of current scientific research is the in-depth study of biologically active compounds and the elucidation of their mechanisms of action on living organisms. From this perspective, aromatic carboxylic acids—and benzoic acid in particular—are among the compounds of significant importance in pharmaceuticals, the food industry, and biological systems. Widely used as an antiseptic and preservative, this substance also attracts interest because it can interact with biologically active molecules [1–5]. Modern computational methods, including molecular docking, are among the most important tools for determining molecular behavior in biological systems [6]. This method allows the determination of binding energy, stability, and optimal configuration between a ligand and a biological target (e.g., a protein) [7]. As a result, it provides essential information about the compound's potential biological activity [8]. In addition, HOMO–LUMO theory plays a central role in studying the electronic structure of a molecule [9]. The energy levels of the HOMO (Highest Occupied Molecular Orbital) and LUMO (Lowest Unoccupied Molecular Orbital) enable assessment of the molecule's chemical reactivity and stability [10]. Furthermore, Molecular Electrostatic Potential (MEP) analysis reveals the electrostatic charge distribution within the molecule, allowing the identification of reactive centers (electrophilic and nucleophilic attack sites) [11]. Atoms in Molecules (AIM) theory is widely used to deepen understanding of intermolecular interactions [12]. This approach enables determination of bond nature and molecular stability through topological analysis of electron-density distribution [13]. Experimentally, vibrational spectroscopy—particularly Raman spectroscopy—is important for determining the structural and dynamic properties of molecules [14]. Raman spectra provide precise information about the bonds, functional groups, and intermolecular interactions within a molecule [15].

In this work, we comprehensively study the molecular properties of benzoic acid and analyze its interaction with biologically active systems using molecular docking [16]. In addition, the electronic structure and reactivity of the molecule are evaluated using MEP, HOMO–LUMO, and AIM methods, and its vibrational properties are determined based on Raman spectroscopy [17]. Together, these approaches deepen understanding of the compound's physicochemical and biological properties [18].

Cite as: A. Jumabaev, H. Hushvaktov, A. Absanov, A. Norkulov, Z. Ernazarov, L. Bulavin, East Eur. J. Phys. 3, 643 (2026), https://doi.org/10.26565/2312-4334-2026-3-60

2. EXPERIMENTAL AND THEORETICAL METHODS

2.1 Experimental method

We used chemically pure benzoic acid and ethanol mixtures in the liquid state at concentrations of 0.9, 0.7, 0.5, 0.3, and 0.1 mol/L. The samples were further purified according to the procedures described in [19].

All experiments were conducted at room temperature and ambient atmospheric pressure. We recorded benzoic acid and its ethanol solutions at various concentrations on an InVia Raman spectrometer equipped with a diffraction grating of 1200 lines/mm. The acquisition time was 10 s and the spectral resolution was 0.01 cm^{-1}. A Spectrum Stabilized Laser Module (532 nm, 50 mW) was used as the excitation light source. The scattered radiation was recorded using a Renishaw CCD Camera detector.

2.2 Computational method

Quantum-chemical calculations were performed using the Gaussian 09W program [20] at the density functional theory (DFT) level, employing the 6-311++G(d,p) basis set and the B3LYP (Becke–3–Lee–Yang–Parr) hybrid functional [21–22]. Spectral analyses were performed using Origin 8.5 [23], and molecular geometry was optimized using GaussView 6 [24]. Molecular docking calculations were performed using the PyRx platform, employing the AutoDock Vina algorithm.

2.3 Molecular Docking Method

In this study, molecular docking calculations were performed to determine the probable interactions of the benzoic acid molecule with the 5IKR enzyme. The three-dimensional crystal structure of the protein was downloaded from the RCSB Protein Data Bank (PDB ID: 5IKR) and prepared for subsequent calculations. During preparation, crystallographic water molecules were removed, polar hydrogen atoms were added to the protein structure, and appropriate charges were assigned. Benzoic acid was selected as the ligand, and its geometry was optimized by quantum-chemical methods. For docking calculations, the neutral form of benzoic acid was employed. The optimized structure was then converted to the PDBQT format required for docking calculations. Molecular docking calculations were performed using the PyRx platform with the AutoDock Vina algorithm [25]. Grid parameters were set to fully encompass the active site of the enzyme, enabling the identification of probable binding conformations of the ligand. The active site was defined using a grid box centered at X = 23.5 Å, Y = 28.7 Å, and Z = 19.4 Å, with dimensions of 25 × 25 × 25 Å. These parameters ensured complete coverage of the binding pocket and enabled the identification of probable binding conformations of the ligand. The obtained results, including binding energies and ligand–protein interaction types, were visualized and analyzed in detail using the Discovery Studio software [26].

3. RESULTS AND DISCUSSION

3.1. Vibrational Frequency Analysis

In this study, the Raman spectra of benzoic acid (BeAc) and its mixtures with ethanol (EtOH) were investigated over a broad spectral range (500–2000 cm^{-1}). The primary focus of the work was on identifying intermolecular interactions—particularly the formation of hydrogen bonds and their effects on vibrational properties. Raman spectroscopy enables the identification of the internal vibrational modes of molecules, thereby providing insight into their structures and interaction mechanisms [27–28]. The spectrum of pure benzoic acid exhibited a series of well-defined and intense peaks. In particular, the signal at 615 cm^{-1} corresponds to the out-of-plane C–H deformation vibration of the aromatic ring. The peak located near 790 cm^{-1} represents C–H bending vibrations within the ring and is characteristic of aromatic systems [29]. The strong peak observed at 1009 cm^{-1} is associated with the symmetric "breathing" vibration of the ring and serves as an important indicator for identifying the aromatic nucleus [30]. In the mid-frequency region, C–H in-plane vibrations are observed at 1132 cm^{-1}, while C–O bond stretching vibrations of the carboxyl group appear at 1288 cm^{-1}. C–H deformation at 1442 cm^{-1} and C=C vibrations of the aromatic ring at 1608 cm^{-1} are also recorded. These results confirm that the aromatic structure and functional groups of the molecule are preserved in their original state [31]. Upon addition of ethanol, significant changes were observed in the spectrum. In the low-frequency region (618–628 cm^{-1} and 792–799 cm^{-1}), the peaks remain essentially unchanged, indicating that the aromatic ring is stable with respect to external perturbations. However, a downshift of the main peak at 1009 cm^{-1} to the 990–1003 cm^{-1} range was observed. This red shift indicates an intensification of intermolecular interactions, specifically the formation of hydrogen bonds [32]. A similar phenomenon is observed in the 1080–1092 cm^{-1} region, where the positions of the C–C and C–O bond vibrations undergo slight changes—evidence for the redistribution of electron density within the system. The C–O stretching vibrations in the 1270–1280 cm^{-1} range show the most pronounced changes: the shift and increase in intensity of these peaks indicate the formation of hydrogen bonds between benzoic acid and ethanol molecules [33]. In the high-frequency region, particularly in the 1448–1457 cm^{-1} range, peak intensities increase, confirming the participation of ethanol molecules in the mixture. At the same time, the aromatic C=C vibrations in the 1600–1608 cm^{-1} range remain virtually unchanged. This result indicates that the interaction occurs predominantly around the carboxyl group, while the aromatic ring remains structurally nearly unaffected [34].

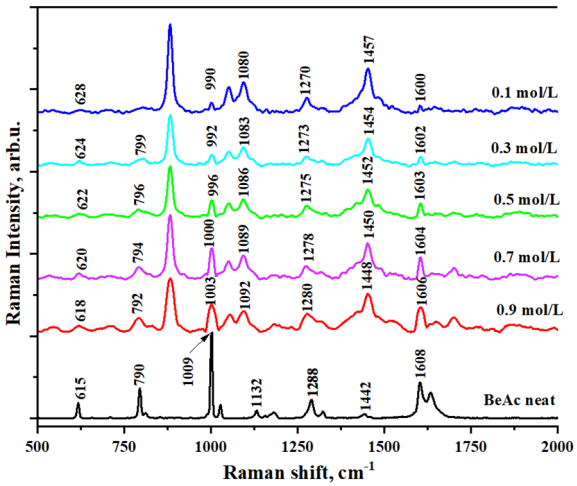

Figure 1. Raman scattering spectra of benzoic acid (BeAc) and its ethanol solutions in the 500–2000 cm^{-1} range

Within the scope of this study, the intermolecular interactions and solvation processes occurring in the binary benzoic acid–ethanol system were thoroughly investigated by Raman spectroscopy (2800–3200 cm^{-1} region), and it was scientifically demonstrated that the observed changes in this system are not merely the result of physical mixing, but rather a consequence of complex thermodynamic and structural reorganization, as evidenced by the following primary mechanisms: (1) Observation of polarization and red-shift in aromatic C–H bonds. In the spectrum of the pure aromatic compound, the peak at 3074 cm^{-1}—characteristic of the stretching vibrations of the =C–H bonds of the benzene ring and observed with high intensity—was found to gradually shift toward lower wavenumbers, reaching 3066 cm^{-1}, as ethanol was added to the system and as the concentration of the solution was progressively diluted (from 0.9 mol/L to 0.1 mol/L). This spectral shift is directly attributed to the disruption of the stable dimer structures formed by benzoic acid molecules and the subsequent formation of a completely new solvation shell involving ethanol molecules, because when the hydroxyl groups of ethanol actively interact with the π-electron cloud of the aromatic ring and with the carboxyl group, the electron density of the =C–H bond is redistributed, and the vibrational energy of this bond decreases appreciably. (2) Dynamics of aliphatic chains and reorganization of solvent microstructure. The 2920–2980 cm^{-1} region of the obtained spectra directly reflects the symmetric and asymmetric stretching vibrations of the $–CH_3$ and $–CH_2$ groups of the ethanol molecule. A change in acid concentration strongly affects the regional distribution of these aliphatic vibrations: in particular, the strong peaks observed at 2930 cm^{-1} and 2975 cm^{-1} at a concentration of 0.9 mol/L were found to shift to 2922 cm^{-1} and 2964 cm^{-1}, respectively, as the system was diluted to 0.1 mol/L. This microdynamics demonstrates that the characteristic macrostructural hydrogen bond network of ethanol is disrupted under the influence of the solute and transitions to a new energetic environment; that is, as the acid content increases, ethanol molecules tend to cluster around acid molecules rather than forming mutual associates, which in turn leads to an increase in steric hindrance and a redistribution of vibrational frequencies in the microenvironment.

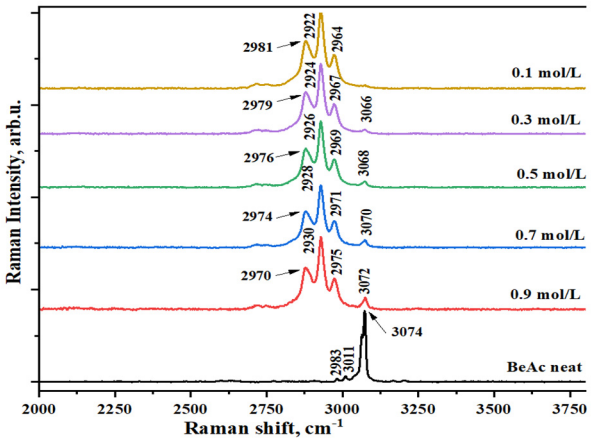

Figure 2. Raman scattering spectra of benzoic acid (BeAc) and its ethanol solutions in the 2000–3800 cm^{-1} range

3.2 Molecular Electrostatic Potential (MEP)

The molecular electrostatic potential (MEP), also known as the molecular potential surface map, is useful for visualizing the charge distribution in benzoic acid and its ethanol complexes, as well as for studying charge-dependent

parameters such as electrophilic–nucleophilic processes and bonding interactions. Determining the MEP helps identify the reactive sites of the molecule [35–37]. Figure 3 presents the MEP visualized using a color-coded scheme. Regions are colored according to the level of electrostatic potential, increasing in the order: deep red < yellow < green < blue [38]. The molecular electrostatic potential (MEP) surface maps visually represent the charge distribution in the benzoic acid monomer, dimer, and benzoic acid + ethanol complexes. They play an important role in studying charge-dependent parameters such as electrophilic and nucleophilic reactions and bonding. An additional purpose of determining the electrostatic potential is to identify the reactive regions of the molecule. The MEP map in the range of -4.389×10^{-2} eV to $+4.389 \times 10^{-2}$ eV clearly shows the charge distribution in the benzoic acid monomer. The oxygen atoms of the carboxyl (C=O) group appear in the deepest red, indicating a higher concentration of electrons—this region is therefore nucleophilic. Yellow regions are moderately electron-rich, green regions are nearly neutral, and blue regions represent electron-deficient electrophilic sites. Regarding vibrations, stretching vibrations of the C=O and O–H bonds, as well as intra-ring C–C bond vibrations, are predominantly observed. The MEP map in the range of -3.127×10^{-2} eV to $+3.127 \times 10^{-2}$ eV shows the redistribution of charges in the benzoic acid dimer. The oxygen atoms of the carboxyl (C=O) group again appear in red, indicating an electron-rich (nucleophilic) region. The intensification of colors between the two molecules reflects their mutual attraction and the formation of hydrogen bonds. Blue regions are electron-deficient and possess electrophilic character. In this configuration, the vibrations also change: in particular, the O–H bond is elongated due to hydrogen bond formation, causing a downshift in its vibrational frequency, and the C=O vibration shifts slightly as well. The MEP map in the range of -3.841×10^{-2} eV to $+3.841 \times 10^{-2}$ eV shows the charge distribution in the benzoic acid + 1 ethanol complex. The oxygen atoms of the carboxyl (C=O) group appear in the deepest red, indicating an electron-rich nucleophilic region. The hydrogen of the –OH group of ethanol is relatively positive, and it is precisely between these two sites that a hydrogen bond forms. The color gradient (red–yellow–green–blue) represents a gradual decrease in charge density: yellow regions are intermediate, green regions are nearly neutral, and blue regions are electron-deficient electrophilic zones. As a result of this interaction, the vibrations of the O–H and C=O bonds shift slightly, confirming the formation of the complex. The MEP map in the range of -5.464×10^{-2} eV to $+5.464 \times 10^{-2}$ eV shows an even stronger redistribution of charges in the complex involving benzoic acid and 2 ethanol molecules. The oxygen atoms of the carboxyl (C=O) group appear in the deepest red, confirming that they constitute the primary nucleophilic center. The hydrogens of the –OH groups of the two ethanol molecules are more positive, and the formation of multiple hydrogen bonds through them is clearly visible. The color gradient (red–yellow–green–blue) illustrates a stepwise decrease in charge density: yellow regions are intermediate, green regions are nearly neutral, and blue regions are electron-deficient electrophilic zones. Consequently, the intermolecular interactions in this complex are stronger, and the vibrations of the O–H and C=O bonds shift considerably.

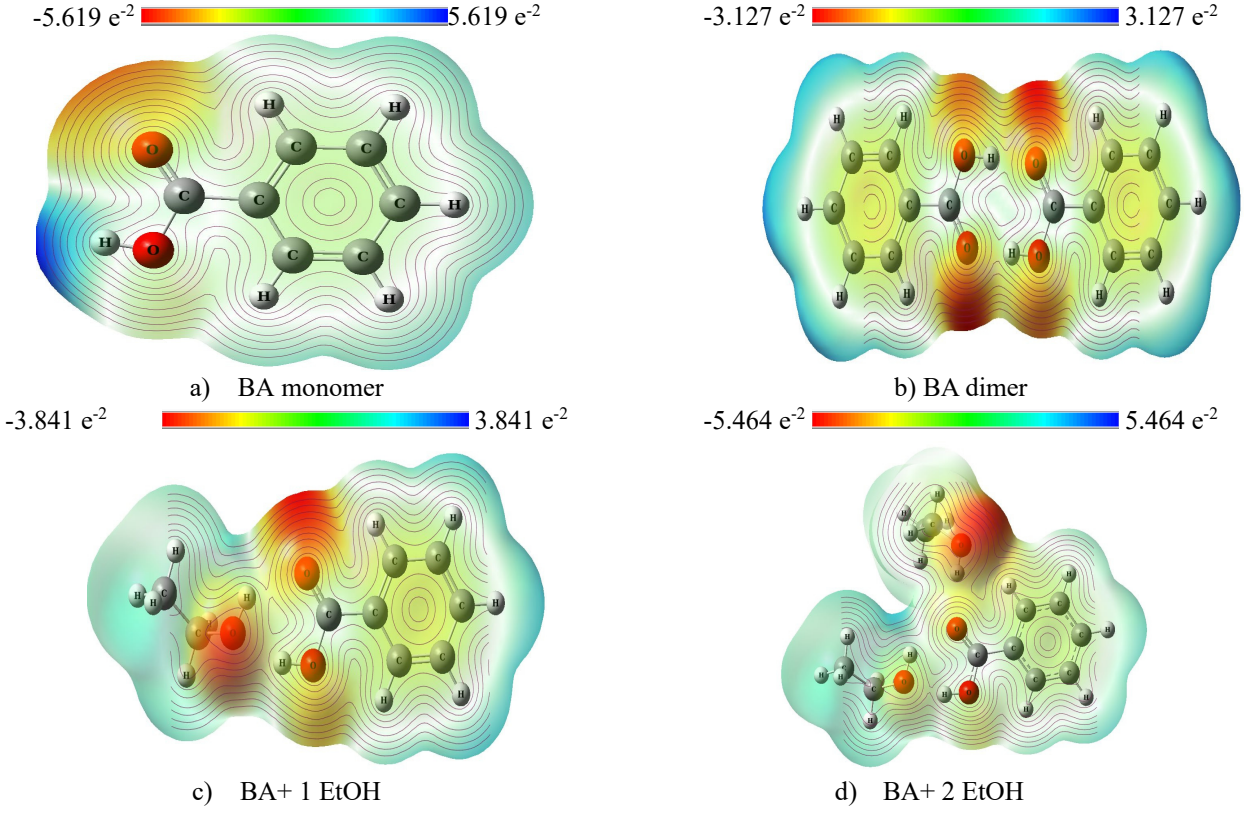

Figure 3. MEP diagram for Benzoic Acid (BA) + Ethanol complexes

3.3 Frontier Molecular Orbital (FMO) Analysis

Frontier molecular orbitals are regarded as important theoretical parameters for interpreting the electronic structure of molecules and their chemical reactivity. The Highest Occupied Molecular Orbital (HOMO) and the Lowest Unoccupied Molecular Orbital (LUMO) describe the outer electronic configuration of the molecule and are of fundamental significance in explaining the mechanisms of reactions involving electron transfer. The HOMO energy level reflects the electron-donating capability of the molecule. If the HOMO energy is relatively high, such molecules readily participate as electron donors and exhibit high activity in nucleophilic or oxidation processes. The LUMO, in contrast, is considered the orbital most susceptible to electron acceptance. If the energy level of this orbital is low, the molecule is well-positioned to accept external electrons and may effectively participate in electrophilic reactions [39–40]. Accordingly, the energy gap (ΔE) between the HOMO and LUMO orbitals is considered one of the primary indicators for assessing the reactivity and stability of a molecular system. A small energy gap indicates high sensitivity of the molecule to external perturbations—particularly electronic excitation—reflecting its greater participation in chemical processes. Conversely, a large ΔE value implies a lower probability of electron transfer, indicating that the molecular system is relatively stable and less reactive. Frontier molecular orbital theory is one of the most widely used quantum-chemical approaches for studying the electronic, optical, and chemical properties of molecules [41]. Based on HOMO and LUMO energy values, a number of global reactivity parameters can also be determined. For instance, chemical hardness (η) is expressed through the difference between HOMO and LUMO energies as:

$$\eta = \frac{E_{LUMO} - E_{HOMO}}{2} \tag{1}$$

This parameter characterizes the resistance of the molecular system to electronic perturbations. Chemical potential (μ) is determined from the following relation:

$$\mu = -\frac{E_{HOMO} + E_{LUMO}}{2} \tag{2}$$

This quantity reflects the tendency of the molecule to attract or donate electrons. Based on these parameters, the electrophilicity index (ω) is also calculated:

$$\omega = \frac{\mu^2}{2\eta} \tag{3}$$

The electrophilicity index is an important indicator for evaluating the electron-accepting capability of the molecule.

Figure 4 displays the spatial distribution of HOMO and LUMO orbitals and the energy gap (ΔE) between them for the benzoic acid molecule and its complexes with ethanol. Table 1 presents the quantum-chemical parameters determined on the basis of HOMO and LUMO energy values, including chemical hardness (η), softness (S), electrophilicity index (ω), and electronegativity (χ). Analysis of the obtained results shows that the benzoic acid + 2 ethanol complex possesses the largest dipole moment, indicating that the intermolecular interactions in this system are relatively strong. In contrast, the benzoic acid + 1 ethanol complex exhibits a lower dipole moment, reflecting a relatively weaker degree of polarization in the system.

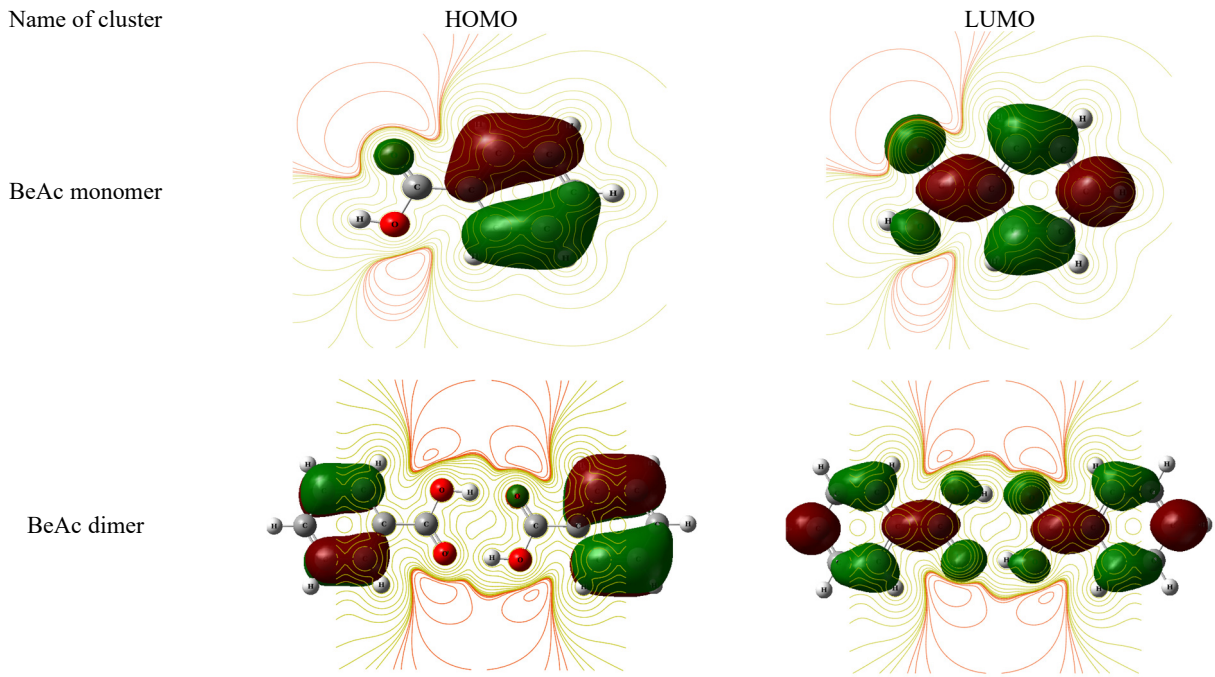

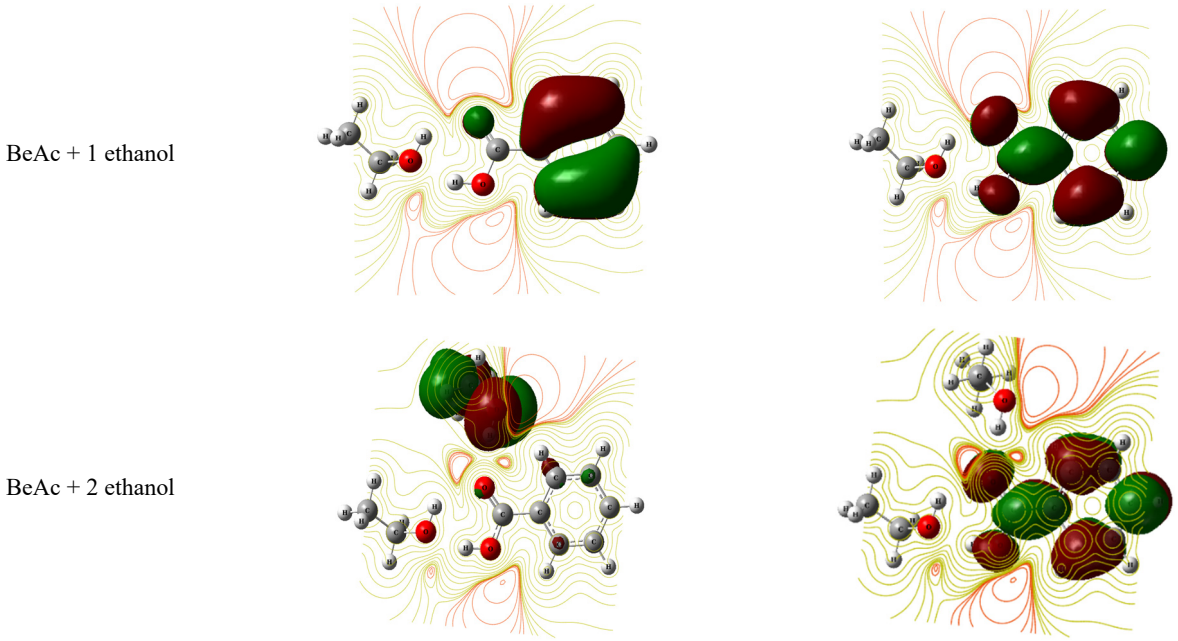

Figure 4. Frontier molecular orbital diagram of benzoic acid and its solutions

The HOMO–LUMO energy gap is one of the key indicators characterizing the electronic structure and chemical stability of a molecule. According to the calculation results, the HOMO–LUMO energy gap for the benzoic acid monomer is 130.32 kcal/mol, and in the dimer form this value is 129.45 kcal/mol. In the complexes formed with a solvent, this parameter was found to be 130.58 kcal/mol for benzoic acid + 1 ethanol, and 123.2 kcal/mol for the benzoic acid + 2 ethanol complex. The ionization potential was also analyzed, with values of 172.11 kcal/mol (benzoic acid monomer), 173.34 kcal/mol (benzoic acid dimer), 169.35 kcal/mol (benzoic acid + 1 ethanol), and 164.86 kcal/mol (benzoic acid + 2 ethanol), respectively. Furthermore, the largest value of the electrophilicity index was found to be 101.8367 kcal/mol, belonging to the benzoic acid monomer.

Table 1. Thermodynamic and chemical parameters of the title compounds

Parameters	BeAc monomer	BeAc dimer	BeAc + 1Ethanol	BeAc + 2Ethanol
Dipole moment (Debye) μ	2.126105	0.005329	1.190733	2.624885
Total energy (Thermal) (kcal/mol)	76.731	155.274	131.706	186.431
Zero-point vibrational energy (kcal/mol)	72.24695	145.47773	123.78239	174.65551
E_{HOMO}	-172.11	-173.34	-169.35	-164.86
E_{LUMO}	-41.79	-43.89	-38.77	-41.66
E_{LUMO} - E_{HOMO}	130.32	129.45	130.58	123.2
Global hardness (η) = ½(E_{LUMO}-E_{HOMO})	56.16	64.725	65.29	61.6
Chemical potential (μ) = ½(E_{LUMO}+E_{HOMO})	-106.95	-108.61	-104.06	-103.26
IP = -E_{HOMO}	172.11	173.34	169.35	164.86
EA = -E_{LUMO}	41.79	43.89	38.77	41.66
Electrophilicity index (ω) = $\mu^2/2\eta$	101.8367	91.1250	82.9260	86.5473

3.4 Atoms in Molecules (AIM) Analysis for Complexes of Benzoic Acid

Atoms in molecules (AIM) analysis is widely used to identify non-covalent interactions in molecular systems [42]. As a result of interactions between two atoms through electron density, a bond path emerges, giving rise to critical points (CPs) in the electron density. At such points, the gradient of the electron density vanishes [43]. The presence of hydrogen bonds or other interactions in molecular complexes is confirmed through the topological analysis of electron density. Figure 5 presents topological parameters for the BeAc dimer, BeAc + 1 ethanol, and BeAc + 2 ethanol complexes: the electron density ρ(r), the Laplacian of the electron density $\nabla^2\rho(r)$, the energy density H(r), the Lagrangian kinetic energy density G(r), and the potential energy density V(r) at the bond critical points (BCPs). These quantities provide extensive information about the nature of the interactions (Table 2).

According to the data presented in Table 2, the Laplacian of the electron density $\nabla^2\rho(r)$ varies in the following ranges: 0.1386–0.1388 a.u. for the BeAc dimer, 0.0681–0.1249 a.u. for BeAc + 1 ethanol, and 0.0328–0.1304 a.u. for BeAc + 2 ethanol. These positive values indicate a local depletion of electron density, confirming that the intermolecular interactions belong to the closed-shell type and are characterized by hydrogen bonds.

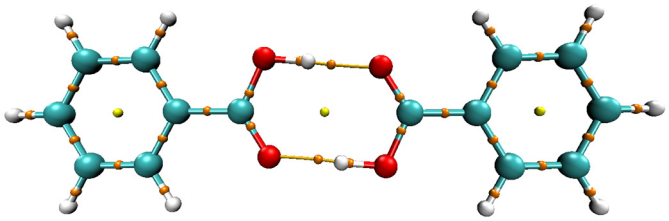

a) BeAc dimer

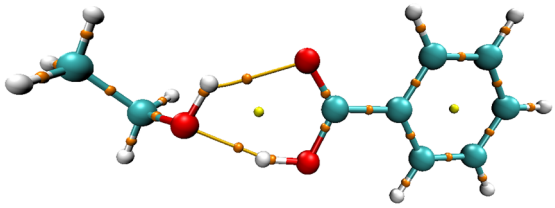

b) BeAc + 1 ethanol

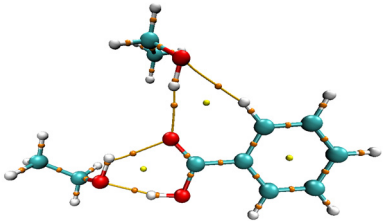

c) BeAc + 2 ethanol

Figure 5. Molecular diagrams of the title complexes. (a) BeAc dimer; (b) BeAc + 1 ethanol; (c) BeAc + 2 ethanol

Table 2. Topological parameters of the title complexes (BeAc, BeAc + ethanol)

Name of cluster	X(H)-bonds	Bond length *r, Å*	Density of all electrons $\rho(r)$	Lagrangian kinetic energy *G(r)*	Potential energy density *V(r)*	Energy density *H(r)*	Laplacian of electron density $\nabla^2\rho(r)$	Bond energy $E_{int} \approx -V(r)/2$, kcal/mol
BeAc dimer	2(O)…30(H)	1.66415	0.0478	0.0401	-0.0455	0.0054	0.1386	14.2758
	15(H)…23(O)	1.66337	0.0479	0.0402	-0.0456	0.0054	0.1388	14.2758
BeAc + 1 ethanol	2(O)…24(H)	2.01938	0.0232	0.0186	-0.0169	0.0016	0.0807	5.3023
	15(H)…16(O)	1.75013	0.0398	0.0334	-0.0356	0.0021	0.1249	11.1696
BeAc + 2 ethanol	2(O)…24(H)	2.10706	0.0196	0.0155	-0.0139	0.0015	0.0681	4.3612
	2(O)…33(H)	1.92863	0.0241	0.0209	-0.0183	0.0026	0.0940	5.7417
	10(H)…25(O)	2.42144	0.0091	0.0068	-0.0054	0.0013	0.0328	1.6942
	15(H)…16(O)	1.72156	0.0424	0.0357	-0.0389	0.0031	0.1304	12.2051

The energy density H(r) values for the BeAc dimer and its ethanol complexes are observed in different ranges: 0.0054 a.u. for the dimer, 0.0015–0.0021 a.u. for complexes with one ethanol molecule, and 0.0013–0.0031 a.u. for systems involving two ethanol molecules. The positive values of H(r) in all cases indicate that the interactions present in these systems are not covalent but rather predominantly electrostatic in nature. This further confirms that they are closed-shell type interactions mediated by hydrogen bonds. This substantiates the existence of weak hydrogen bonds between the presented complexes [44–45]. Such hydrogen bonds are analogous in nature to van der Waals interactions. The formula $E_{int} = V(r)/2$ was used to calculate the bond energy [46]. In this work, it was applied to determine hydrogen bond energies, where V(r) is the potential energy density at the bond critical points. If the energy density value at the critical points is negative ($H_{DCP_s} < 0$), the bond has covalent character; if positive ($H_{DCP_s} > 0$), it has electrostatic character.

3.5. Molecular Docking

Molecular docking is one of the modern computational approaches for modeling interactions between biomolecules. In this method, the protein is treated as a receptor and the small molecule as a ligand, and their binding characteristics and stability are evaluated. The degree of binding is typically expressed in terms of free energy values [47]. The Swiss Target Prediction method was used to identify the target protein for molecular docking studies [48]. In this work, the benzoic acid molecule was selected as the ligand, and molecular docking analysis was performed to evaluate its biological activity. Cyclooxygenase-2 (PDB ID: 5IKR) was used as the target protein for the study. This protein is associated with inflammatory processes and is one of the important biological targets extensively studied in pharmaceutical research. Docking results showed that the benzoic acid molecule is accommodated appropriately within the active site of the protein

and forms several significant interactions. The best binding pose exhibited a binding affinity of −5.8 kcal/mol, indicating favorable interaction between benzoic acid and the active site of the protein.

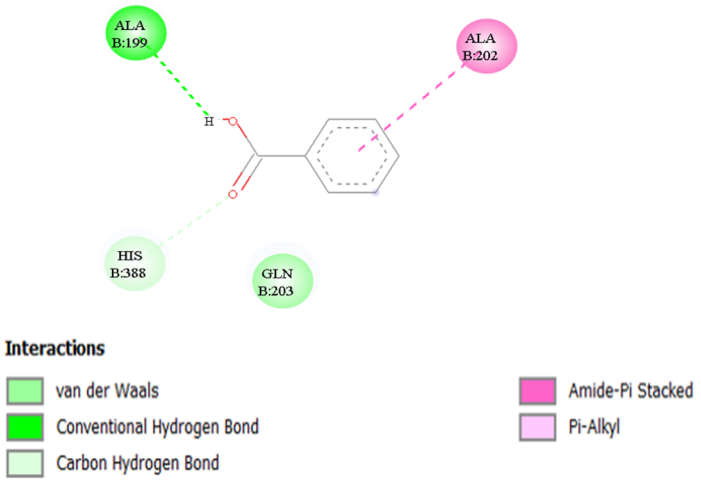

Figure 6. 2D interaction diagram of benzoic acid within the active site of the 5IKR protein

In particular, the hydrogen bond formed with the ALA (B:199) residue contributes significantly to the stability of the complex. The hydrogen-bond distance was estimated to be approximately 2.04 Å, indicating a relatively stable intermolecular interaction. Additionally, a hydrophobic π-alkyl interaction between the aromatic ring of the ligand and ALA (B:202) was observed. Furthermore, weak interactions—including van der Waals contacts and carbon–hydrogen bonds—were identified with the HIS (B:388) and GLN (B:203) amino acid residues. Such interactions contribute to the overall energetic stability of the complex. To provide a broader assessment of the docking results, the co-crystallized ligand mefenamic acid (ID8) was used as a reference molecule. Benzoic acid retained a favorable orientation within the binding cavity and formed intermolecular contacts that contributed to the stability of the resulting complex. The inclusion of the co-crystallized ligand as a reference molecule provided additional confidence in the reliability of the docking results and the predicted binding mode of benzoic acid. In general, the results demonstrate that the benzoic acid molecule possesses the capacity to bind to the 5IKR protein. This allows it to be considered as a potentially biologically active compound. However, additional experimental and theoretical investigations are required to reach more definitive conclusions.

a) ***b)***

Figure 7. (a) Overview of the 5IKR protein; (b) 3D interaction of benzoic acid with the 5IKR protein

This figure shows the three-dimensional binding pose of benzoic acid within the active site of Cyclooxygenase-2 (PDB ID: 5IKR). The interaction between the ligand and the protein is represented through hydrogen bond donor (pink) and acceptor (green) regions, illustrating how it accommodates within the active site. As seen from the figure, the functional groups of benzoic acid are positioned in close proximity to specific amino acid residues of the protein, forming weak yet relatively stable interactions with them. In particular, hydrogen bonds formed through the carboxyl group make a significant contribution to the spatial stability of the complex. Moreover, the donor and acceptor surfaces generated around the ligand are related to its electron density distribution, which enhances its compatibility with the active site and increases the probability of binding. These results confirm the existence of interactions between benzoic acid and the 5IKR protein and demonstrate its potential biological activity.

4. CONCLUSIONS

In this work, we investigated the intermolecular interactions in benzoic acid and ethanol mixtures in detail using Raman spectroscopy. Analysis of spectra from solutions prepared at various mole fractions showed significant shifts in

the principal vibrational bands due to changes in the solvent environment and, in particular, hydrogen-bond formation. Specifically, the shift of the vibrational mode of the aromatic ring of benzoic acid—characteristic at ~1009 cm^{-1}—toward lower frequencies (990–1003 cm^{-1}) unambiguously indicates the presence of intermolecular interactions. Additionally, shifts in the vibrations associated with C–O and O–H bonds, along with changes in their intensities, confirm complex formation. The analyses show that the aromatic ring structure remains virtually unchanged—that is, it is stable with respect to external perturbations. Conversely, the principal changes occur around the carboxyl functional group, identifying this region as the primary center of intermolecular interaction.

The quantum-chemical results fully corroborated the experimental observations. DFT calculations determined the electronic structure, charge distribution, and energetic parameters of the molecules, showing that electron density redistributes during complex formation. MEP maps identified the most reactive sites: the oxygen atoms of the carboxyl group participate as electron-rich (nucleophilic) centers, while the hydrogen of the –OH group of ethanol acts as a positive (electrophilic) center. HOMO–LUMO analysis revealed a decrease in the energy gap, indicating increased reactivity—an effect that intensifies as the number of ethanol molecules increases. AIM results provided an even more precise picture of the intermolecular interactions. The calculated parameters demonstrated that these bonds are non-covalent, being primarily electrostatic and characterized by weak hydrogen bonding. This indicates the predominance of closed-shell type interactions within the system. Molecular docking analysis allowed us to evaluate benzoic acid's ability to interact with biological systems. The results showed that it can form a stable complex with the Cyclooxygenase-2 (5IKR) protein, in which hydrogen bonds and hydrophobic interactions play a crucial role. This confirms the molecule's potential biological activity.

In conclusion, the investigations showed that intermolecular interactions in the benzoic acid–ethanol system are mediated primarily through hydrogen bonds, and that this process significantly influences the molecule's vibrational properties, electronic structure, and reactivity. The results are important not only for understanding the physicochemical properties of this system, but also for elucidating the molecule's behavior in a biological environment.

ORCID

Abduvakhid Jumabaev, https://orcid.org/0000-0002-4817-0290; **Hakim Hushvaktov,** https://orcid.org/0000-0001-9149-754X;
Asliddin Norkulov, https://orcid.org/0009-0008-2832-5962; **Leonid Bulavin,** https://orcid.org/0000-0002-8063-6441

REFERENCES

[1] Howard, D. L., Kjaergaard, H. G., Huang, J., & Meuwly, M. Infrared and near-infrared spectroscopy of acetylacetone and hexafluoroacetylacetone. The Journal of Physical Chemistry A, **119**(29), 7980–7990 (2015). https://doi.org/10.1021/acs.jpca.5b01863

[2] Trivella, A., Wassermann, T. N., Mestdagh, J. M., Tanner, C. M., Marinelli, F., Roubin, P., & Coussan, S. New insights into the photodynamics of acetylacetone: isomerization and fragmentation in low-temperature matrixes. Physical Chemistry Chemical Physics, **12**(29), 8300–8310 (2010). https://doi.org/10.1039/C003593A

[3] Jumabaev, A., Koyambo-Konzapa, S. J., Hushvaktov, H., Absanov, A., Khudaykulov, B., Holikulov, U., et al. Intermolecular interactions in water and ethanol solution of ethyl acetate: Raman, DFT, MEP, FMO, AIM, NCI-RDG, ELF, and LOL analyses. Journal of Molecular Modeling, **30**(10), 349 (2024). https://doi.org/10.1007/s00894-024-06147-0

[4] Jumabaev A., Absanov A., Ernazarov Z., Shodiyev A., Umarov S. Raman spectra and ab initio calculation analysis of intermolecular interactions in ethyl acetate, Journal of Samarkand State University, **139**(1), 5–12 (2023). https://doi.org/10.59251/2181-1296.2023.v4.139.1.2085

[5] Jumabaev A., Absanov A.A., Khudaykulov B.B., Ernazarov Z.I. Investigation of intermolecular interactions in butyl acetate using vibrational spectroscopy and nonempirical calculations, Uzbek Physical Journal. **25**(4), (2023). https://doi.org/10.52304/.v25i4.471

[6] Pinzi, L., & Rastelli, G. Molecular docking: shifting paradigms in drug discovery. International Journal of Molecular Sciences, **20**(18), 4331 (2019). https://doi.org/10.3390/ijms20184331

[7] Morris, G. M., Huey, R., Lindstrom, W., Sanner, M. F., Belew, R. K., Goodsell, D. S., & Olson, A. J. AutoDock4 and AutoDockTools4: Automated docking with selective receptor flexibility. Journal of Computational Chemistry, **30**(16), 2785–2791. https://doi.org/10.1002/jcc.21256

[8] Trott, O., & Olson, A. J. (2010). AutoDock Vina: improving the speed and accuracy of docking with a new scoring function, efficient optimization, and multithreading. Journal of Computational Chemistry, **31**(2), 455–461 (2009). https://doi.org/10.1002/jcc.21334

[9] Parr, R. G. *Density functional theory of atoms and molecules. In Horizons of Quantum Chemistry*, (Springer, Dordrecht, Netherlands, 1989), pp. 5–15. https://doi.org/10.1007/978-94-009-9027-2_2

[10] Koopmans, T. Ordering of wave functions and eigenenergies to the individual electrons of an atom, Physica, **1**, 104–113 (1933).

[11] Politzer, P., & Murray, J. S. The fundamental nature and role of the electrostatic potential in atoms and molecules. Theoretical Chemistry Accounts, **108**(3), 134–142 (2002). https://doi.org/10.1007/s00214-002-0363-9

[12] Bader, R. F. Everyman's derivation of the theory of atoms in molecules, The Journal of Physical Chemistry A, **111**(32), 7966-7972 (2007). https://doi.org/10.1021/jp073213k

[13] Koch, D., Pavanello, M., Shao, X., Ihara, M., Ayers, P. W., Matta, C. F., et al. The analysis of electron densities: From basics to emergent applications. Chemical Reviews, **124**(22), 12661–12737 (2024). https://doi.org/10.1021/acs.chemrev.4c00297

[14] John R. Ferraro, Kazuo Nakamoto and Chris W. Brown. *Introductory Raman Spectroscopy*, (Elsevier, 2003).

[15] Ferraro J.R., Nakamoto K., and Brown C.W. *Recent Developments in Atomic Force Microscopy and Raman Spectroscopy for Materials Characterization. Introductory Raman Spectroscopy*, (Academic Press, 2003). http://dx.doi.org/10.5772/intechopen.97257
[16] Daina, A., Michielin, O., & Zoete, V. Swiss Target Prediction: updated data and new features for efficient prediction of protein targets of small molecules. Nucleic Acids Research, **47**(W1), W357–W364 (2019). https://doi.org/10.1093/nar/gkz382
[17] Becke, A. D. Density-functional thermochemistry. III. The role of exact exchange. The Journal of Chemical Physics, **98**(7), 5648-5652 (1993). https://doi.org/10.1063/1.464913
[18] Burke, K. Perspective on density functional theory, The Journal of Chemical Physics, **136**(15), (2012). https://doi.org/10.1063/1.4704546
[19] Gordon, A. G., AND Ford, R. A. *The Chemist's Companion: A Handbook of Practical Data, Techniques, and References*, (Wiley, 1973).
[20] Frisch, M.J. et al. Gaussian 09, Revision D.01. Gaussian, Inc., Wallingford, (2009).
[21] Lee, C., Yang, W., & Parr, R. G. Development of the Colle-Salvetti correlation-energy formula into a functional of the electron density, Physical Review B, **37**(2), 785 (1988). https://doi.org/10.1103/PhysRevB.37.785
[22] Krishnan, R. B. J. S., Binkley, J. S., Seeger, R., & Pople, J. A. Self-consistent molecular orbital methods. XX. A basis set for correlated wave functions, The Journal of Chemical Physics, **72**(1), 650–654 (1980). https://doi.org/10.1063/1.438955
[23] Moberly, J. G., Bernards, M. T., Waynant, K. V. Key features and updates for Origin 2018, J. Cheminform., **10**(5), (2018). https://doi.org/10.1186/s13321-018-0259-x
[24] Dennington, R.; Keith, T. A.; and Millam, J. M. GaussView Version 6.0. Semichem Inc., Shawnee Mission, KS, (2016).
[25] Trott, O., & Olson, A. J. AutoDock Vina. Journal of Computational Chemistry, **31**(2), 455–461 (2010). https://doi.org/10.1002/jcc.21334
[26] Dallakyan, S., & Olson, A. J. Small-molecule library screening by docking with PyRx, in: *Chemical Biology: Methods and Protocols*, (Springer New York, 2014), pp. 243–250. https://doi.org/10.1007/978-1-4939-2269-7_19
[27] Smith, E., & Dent, G. *Modern Raman Spectroscopy: A Practical Approach*, (John Wiley & Sons, (2019).
[28] Kolesov, B. A. Hydrogen bonds: Raman spectroscopic study. International Journal of Molecular Sciences, **22**(10), 5380 (2021). https://doi.org/10.3390/ijms22105380
[29] Socrates, G. *Infrared and Raman Characteristic Group Frequencies: Tables and Charts*, (John Wiley & Sons, 2004).
[30] Ferraro, J. R., Nakamoto, K., Brown, C. W. *Introductory Raman Spectroscopy*, (Academic Press, 2003).
[31] Meenakshi, R. Experimental (FT-IR and FT-Raman) and spectroscopic investigations, electronic properties and conformational analysis. RSC Advances, **6**(26), 21822–21831 (2016). https://doi.org/10.1039/C6RA00092D
[32] Burikov, S., Dolenko, T., Patsaeva, S., Starokurov, Y., & Yuzhakov, V. Raman and IR spectroscopy research on hydrogen bonding in water–ethanol systems. Molecular Physics, **108**(18), 2427–2436 (2010). https://doi.org/10.1080/00268976.2010.516277
[33] Rozenberg, M., Loewenschuss, A., & Marcus, Y. An empirical correlation between stretching vibration redshift and hydrogen bond length. Physical Chemistry Chemical Physics, **2**(12), 2699–2702 (2000). https://doi.org/10.1039/B002216K
[34] Max, J. J., Chapados, C. Infrared spectroscopy of aqueous carboxylic acids. Journal of Chemical Physics, **116**, 4626–4642 (2002). https://doi.org/10.1021/jp036401t
[35] Suresh, C. H., Remya, G. S., & Anjalikrishna, P. K. Molecular electrostatic potential analysis: A powerful tool to interpret and predict chemical reactivity. Wiley Interdisciplinary Reviews: Computational Molecular Science, **12**(5), e1601 (2022). https://doi.org/10.1002/wcms.1601
[36] Koyambo-Konzapa S.-J., Oubella A., Issaoui N., et al., Molecular structure, spectroscopic (FT-IR, NMR and UV–Vis), electronic properties, molecular docking, and molecular dynamics studies on novel thiazolidinone derivative, J. Mol. Struct. **1318**, 139301 (2024). https://doi.org/10.1016/j.molstruc.2024.139301
[37] Jumabaev, A. et al. Insights into Amyl Acetate–Chloroform Interactions: Vibrational Spectroscopy and Quantum Topology Study. Ukrainian Journal of Physics, **71**(1), 28–38 (2026). https://doi.org/10.15407/ujpe71.1.28
[38] Jumabaev, A. et al. Vibrational spectra and computational study of amyl acetate: MEP, AIM, RDG, NCI, ELF, and LOL analysis. Ukr. J. Phys. **69**, 742 (2024). https://doi.org/10.15407/ujpe69.10.742
[39] Jalbout, A. F., Trzaskowski, B., & Hameed, A. J. Theoretical investigation of the electronic structure of 1-(3,4;3,5 and 3,6-bis-selenocyanato-phenyl)pyrrolidinofullerenes. Journal of Organometallic Chemistry, **691**(22), 4589–4594 (2006). https://doi.org/10.1016/j.jorganchem.2006.06.041
[40] Jalbout, A. F., Hameed, A. J., & Trzaskowski, B. Study of the structural and electronic properties of 1-(4,5 and 6-selenenyl derivatives-3-formyl-phenyl)pyrrolidinofullerenes. Journal of Organometallic Chemistry, **692**(5), 1039–1047 (2007). https://doi.org/10.1016/j.jorganchem.2006.10.068
[41] Khudaykulov, B., Norkulov, A., Holikulov, U., Absanov, A., Doroshenko, I., & Jumabaev, A. Raman and DFT study of non-covalent interactions in liquid benzophenone and its solutions. Low Temperature Physics, **51**(2), 220–230 (2025). https://doi.org/10.1063/10.0035406
[42] Akman, F., Issaoui, N., & Kazachenko, A. S. Intermolecular hydrogen bond interactions in the thiourea/water complexes: X-ray, DFT, NBO, AIM, and RDG analyses. Journal of Molecular Modeling, **26**(6), 161 (2020). https://doi.org/10.1007/s00894-020-04423-3
[43] Bader, R. F. Definition of molecular structure: by choice or by appeal to observation? The Journal of Physical Chemistry A, **114**(28), 7431–7444 (2010). https://doi.org/10.1021/jp102748b
[44] Rozas, I., Alkorta, I., & Elguero, J. Behavior of ylides containing N, O, and C atoms as hydrogen bond acceptors. Journal of the American Chemical Society, **122**(45), 11154–11161 (2000). https://doi.org/10.1021/ja0017864
[45] Tang, T. H., Deretey, E., Knak Jensen, S. J., & Csizmadia, I. G. Hydrogen bonds: Relation between lengths and electron densities at bond critical points. The European Physical Journal D, **37**(2), 217–222 (2006). https://doi.org/10.1140/epjd/e2005-00317-0
[46] Espinosa, E., Molins, E., & Lecomte, C. Hydrogen bond strengths revealed by topological analyses of experimentally observed electron densities. Chemical Physics Letters, **285**(3–4), 170–173 (1998). https://doi.org/10.1016/S0009-2614(98)00036-0

[47] Pinzi, L., & Rastelli, G. Molecular docking: shifting paradigms in drug discovery. International Journal of Molecular Sciences, **20**(18), 4331 (2019). https://doi.org/10.3390/ijms20184331
[48] Daina, A., Michielin, O., & Zoete, V. SwissTargetPrediction: updated data and new features for efficient prediction of protein targets of small molecules. Nucleic Acids Research, **47**(W1), W357–W364 (2019). https://doi.org/10.1093/nar/gkz382

ЕЛЕКТРОННА СТРУКТУРА ТА МІЖМОЛЕКУЛЯРНІ ВЗАЄМОДІЇ КОМПЛЕКСУ БЕНЗОЙНА КИСЛОТА–ЕТАНОЛ: СПЕКТРОСКОПІЯ КОРОБІНАЦІЙНОГО РАЗМІНУ, ДПФ ТА АНАЛІЗ МОЛЕКУЛЯРНОГО ДОКІНГУ

Абдувахід Джумабаєв[1], Хакім Хушвактов[1], Ахмад Абсанов[1], Асліддін Норкулов[1], Зохід Ерназаров[1], Леонід Булавін[2]
[1]Самаркандський державний університет імені Шарофа Рашидова,
140104, м. Самарканд, Узбекистан, Університетський бульвар, 15;
[2]Київський національний університет імені Тараса Шевченка (вул. Володимирська, 64/13, Київ 01601, Україна)

У цій роботі ми досліджували міжмолекулярні взаємодії в бензойній кислоті та її етанольних розчинах за допомогою раманівської спектроскопії та квантово-хімічних підходів. Аналіз спектрів комбінаційного розсіювання показав, що додавання етанолу викликає значні зміни в коливальному спектрі бензойної кислоти. Ці зміни в першу чергу зумовлені ефектами розчинника та утворенням водневих зв'язків і найбільш виражені в режимах коливань, що відповідають карбоксильній групі. Майже інваріантність ароматичного кільця підтверджує збереження структурної цілісності молекули. Теоретичні розрахунки були виконані на рівні DFT, що забезпечує ретельний аналіз електронної структури та енергетичних характеристик системи. Поверхню молекулярного електростатичного потенціалу (MEP) використовували для ідентифікації реакційноздатних центрів у молекулі; атоми кисню карбоксильної групи виникли як основні багаті електронами нуклеофільні центри, тоді як група –OH етанолу відіграла значну роль у формуванні водневих зв'язків. Орбітальний аналіз HOMO–LUMO продемонстрував перерозподіл електронної густини під час утворення комплексу та збільшення реакційної здатності системи. Результати молекулярного докінгу також підтвердили здатність бензойної кислоти взаємодіяти з біологічно активним сайтом зв'язування. Під час розрахунків молекула прийняла стабільну конформацію в межах активного центру білка, утворюючи комплекс через водневі зв'язки та інші слабкі міжмолекулярні взаємодії. Ці висновки узгоджуються з MEP та аналізом електронної структури, демонструючи тісний зв'язок між квантово-хімічними властивостями молекули та її потенційною біологічною активністю. Дослідження розкривають механізм міжмолекулярних взаємодій у системі бензойна кислота–етанол і дають вичерпне пояснення того, як ці взаємодії впливають на коливальні властивості молекули, електронну структуру та поведінку в біологічному середовищі.

Ключові слова: *раманівська спектроскопія; ab initio розрахунки; водневий зв'язок; бензойна кислота; етанол; поверхня молекулярного електростатичного потенціалу (МЕП); AIM; FMO; молекулярний докінг*